ISSN 0915-633X

NATIONAL INSTITUTE FOR FUSION SCIENCE

Chaotic Transients and Fractal Structures Governing Coupled Swing Dynamics

Y. Ueda, T. Enomoto and H. B. Stewart

(Received – Sep. 20, 1990)

NIFS-55 Oct. 1990

RESEARCH REPORT
NIFS Series

NAGOYA, JAPAN

Submitted to EPRI Workshop on Applications of Chaos, December 1990.

Chaotic transients and fractal structures governing coupled swing dynamics*

Y. UEDA and T. ENOMOTO

Department of Electrical Engineering
Kyoto University
Kyoto 606, Japan

and

H. B. STEWART

Mathematical Sciences Group
Department of Applied Science
Brookhaven National Laboratory
Upton, NY 11973

Numerical simulations are used to study coupled swing equations modeling the dynamics of two electric generators connected to an infinite bus by a simple transmission network. In particular, the effect of varying parameters corresponding to the input power supplied to each generator is studied. In addition to stable steady operating conditions, which should correspond to synchronized, normal operation, the coupled swing model has other stable states of large amplitude oscillations which, if realized, would represent non-synchronized motions: the phase space boundary separating their basins of attraction is fractal, corresponding to chaotic transient motions. These fractal structures in phase space and the associated fractal structures in parameter space will be of primary concern to engineers in predicting system behavior.

*This work was supported by the Applied Mathematical Sciences program of the U.S. Department of Energy under Contract No. DE-AC02-76CH00016.

1. Introduction

The stability of electric power systems has a long history of research. The question of transient stability has been studied primarily by examining solutions of systems of differential equations based on the swing equation, or driven pendulum. Almost all research has relied on application of an energy-integral or Lyapunov function to determine stability in a neighborhood of a desired solution; see for example references [1], [2], [3]. Although these methods may give sufficient conditions for practical operation, this approach by its nature does not address the question of the global structure in phase space of the basin of attraction of the desired stable operating condition, and it seems possible that an additional margin of safety may exist which cannot be identified by existing approaches. In any case, it is the basin of attraction which represents the proper focus of concern for the engineer, and this is the problem we shall study here. We note that our focus on basin boundary structure rather than stability near a desired solution closely parallels the new approach to ship stability criteria proposed by Thompson et al [4].

One difficulty with the study of basin structures is their complexity, involving fractal basin boundaries [5]. The geometric theory of dynamic systems, including invariant manifolds, offers conceptual tools which may be helpful in elucidating these fractal structures. Here we make no final judgment on the practical utility of invariant manifold analysis, but simply present it with the aim of clarifying what we feel is the true and proper concern of engineering stability analysis, namely the structure of basins of attractions and their boundaries. The model treated here uses the simplest expression for the generator, although

in applications a more accurate model of the generator should be used. The geometric theory of dynamical systems is very general, and could in principle easily accommodate more realistic models.

We consider a simple model of the dynamics of two electric generators connected to an infinite bus by a simple network consisting of two transmission lines. The configuration of this network is shown in Figure 1. Generator 1 is driven by mechanical input power P_{m1} and delivers its electrical output to transmission line 1 with transfer admittance y_1, while generator 2 with input power P_{m2} delivers its output to transmission line 2 with transfer admittance y_2, which is connected through line 1 to the same load, i.e., infinite bus.

The equations used here to describe the dynamics of this system are

$$\begin{aligned}
\frac{d\delta_1}{dt} &= \omega_1 \\
\frac{d\omega_1}{dt} &= \frac{1}{m_1}\{-d_1\omega_1 + p_1 - \sin(\delta_1 - \delta_2) - k\sin\delta_1\} \\
\frac{d\delta_2}{dt} &= \omega_2 \\
\frac{d\omega_2}{dt} &= \frac{1}{m_2}\{-d_2\omega_2 + p_2 - \sin(\delta_2 - \delta_1)\}
\end{aligned} \tag{1}$$

Here δ_1 and δ_2 are angular positions of the generator rotors, ω_1 and ω_2 the angular velocities; these four state variables of the system are measured relative to the rotating reference of the infinite bus voltage. Both terminal voltages of the generators are regulated to maintain the same voltage as the infinite bus. The quantities p_1 and p_2 are the input powers normalized by the quantity y_2E^2. The d_i are damping coefficients and the m_i are inertia constants, both likewise normalized by y_2E^2; and $k = y_1/y_2$ is equal to the ratio of the admittances of the two transmission lines. These equations are derived under the

assumption of small deviations in the angular frequencies from true $60Hz$ oscillation; but the angular positions make large excursions.

Following the geometric method of Poincaré, we take the four state variables to be the coordinates of a four-dimensional phase space; an initial value is a point in this space, and solutions of the differential equations over time will trace out trajectories or orbits in this phase space. Since we cannot visualize this phase space directly, we shall consider two-dimensional subspaces such as (δ_1, δ_2) for example, and either look at the intersection of trajectories with the subspace, or the projection of trajectories onto the subspace. Note that topologically the phase space is equivalent to the Cartesian product of a torus $(\delta_1, \delta_2) \in S^1 \times S^1 = T^2$ with a plane $(\omega_1, \omega_2) \in R^2$; for the torus we take the usual projection of T^2 unwrapped to the square $[0, 2_\pi) \times [0, 2_\pi)$.

The remaining quantities in the system (1) are parameters, held constant while a given trajectory is solved by integration. In a real power network, the d_i, m_i, and k are fixed characteristics of the network, while the input powers p_i are under the control of the engineer. It is therefore natural that p_1 and p_2 should enjoy a special role; we call them control parameters, or controls. In this study we fix

$$m_1 = m_2 = 0.1$$
$$d_1 = d_2 = 0.005$$
$$k = 1$$

throughout, and consider the effect on solutions of choosing different values of p_1 and p_2. Following the comprehensive geometric viewpoint of Thom[6] and Abraham[7], we consider a control-phase space which is the Cartesian product of the control plane $(p_1, p_2) \in R^2$ with

the phase space. Of particular interest in this study is the occurrence of fractal structure in the control plane, which according to the comprehensive view is a consequence of coherent structure in control-phase space linking the fractal structure in control space with fractal structure in phase space. Here we shall be content with visualizing the phenomenon in the (p_1, p_2) plane and separately, in subspaces of phase space, with hope that the reader will keep in mind the existence of a more comprehensive view; see for example Abraham and Shaw[8] for a visual introduction to the comprehensive view.

2. Regular Basic Motions

The first step in constructing a geometric phase portrait of the system (1) is to find the solutions corresponding to regular motions, that is, the equilibrium points corresponding to steady motions, and the closed trajectories corresponding to periodic motions. In either case the regular motion may be stable or unstable. The stable motions are attractors, motions which can be sustained in a real system. The unstable motions are not typically observed in real systems, but they are nevertheless important in understanding the geometric structure of phase space and the overall dynamical behavior. Of particular interest are the unstable motions which lie in the boundaries separating basins of attraction of the various stable motions.

The equilibrium points of (1) are found by setting all time derivatives

to zero, leading to the conditions

$$\begin{aligned} \omega_1 &= 0 \\ \omega_2 &= 0 \\ k\sin\delta_1 + \sin(\delta_1 - \delta_2) &= p_1 \\ \sin(\delta_2 - \delta_1) &= p_2 \end{aligned} \tag{2}$$

which are to be solved for the state variable coordinates of the equilibrium points. We consider the region of control space

$$\begin{aligned} |p_1 + p_2| &\le k = 1 \\ |p_2| &\le 1 \end{aligned} \tag{3}$$

where there are four fixed point solutions of (2). Clearly $\omega_1 = \omega_2 = 0$ in all cases; the δ_i coordinates are

$$\begin{aligned} \delta_1^{(1)} &= \mathrm{Sin}^{-1}\frac{p_1+p_2}{k} & \delta_2^{(1)} &= \mathrm{Sin}^{-1}p_2 + \mathrm{Sin}^{-1}\frac{p_1+p_2}{k} \\ \delta_1^{(2)} &= \mathrm{Sin}^{-1}\frac{p_1+p_2}{k} & \delta_2^{(2)} &= \pi - \mathrm{Sin}^{-1}p_2 + \mathrm{Sin}^{-1}\frac{p_1+p_2}{k} \\ \delta_1^{(3)} &= \pi - \mathrm{Sin}^{-1}\frac{p_1+p_2}{k} & \delta_2^{(3)} &= \pi + \mathrm{Sin}^{-1}p_2 - \mathrm{Sin}^{-1}\frac{p_1+p_2}{k} \\ \delta_1^{(4)} &= \pi - \mathrm{Sin}^{-1}\frac{p_1+p_2}{k} & \delta_2^{(4)} &= -\mathrm{Sin}^{-1}p_2 - \mathrm{Sin}^{-1}\frac{p_1+p_2}{k}. \end{aligned} \tag{4}$$

Figure 2 shows the locations of these fixed points in the (δ_1, δ_2) plane for the example $p_1 = 0.1$, $p_2 = 0.1$. Clearly fixed point 1 is close to the condition $\delta_1 = \delta_2 = 0$ with no power generated.

The stability of the fixed points is determined by linearizing the system (1) near a fixed point, so that small deviations from the fixed point are governed by the matrix

$$\begin{bmatrix} 0 & 1 & 0 & 0 \\ -\frac{1}{m_1}\cos(\delta_1-\delta_2) - \frac{k}{m_1}\cos\delta_1 & \frac{-d_1}{m_1} & \frac{1}{m_1}\cos(\delta_1-\delta_2) & 0 \\ 0 & 0 & 0 & 1 \\ \frac{1}{m_2}\cos(\delta_2-\delta_1) & 0 & -\frac{1}{m_2}\cos(\delta_2-\delta_1) & -\frac{d_2}{m_2} \end{bmatrix} \tag{5}$$

Table 1 gives numerical values of the coordinates δ_1 and δ_2 of the four fixed points for example $p_1 = 0.1$, $p_2 = 0.1$ illustrated in Figure 2. Also given in Table 1 are the eigenvalues of the matrix (5) for each fixed point. The fixed point 1 has negative real part for all four eigenvalues, and is therefore stable. The remaining three fixed points have at least one positive real eigenvalue and are therefore unstable.

The single positive eigenvalue of fixed points 2 and 3 indicates that near each of these points there is a 3-dimensional subspace within which trajectories approach the fixed point, and a one-dimensional subspace in which trajectories diverge from the fixed point. Well-known theorems establish the fact that these subspaces can be extended to globally defined manifolds in phase space, a 3-dimensional stable manifold or inset, and a one-dimensional unstable manifold or outset. The inset consists of trajectories which are asymptotic to the fixed point as $t \to \infty$. The inset can be located by starting from initial conditions near the fixed point in the 3-dimensional subspace spanned by the three incoming eigenvalues, and integrating such initial conditions backwards in time. The outset consists of two trajectories asymptotic to the fixed point as $t \to -\infty$. That is, each of the fixed points 2 and 3 has an outset consisting of two branches. The local inset of each fixed point separates trajectories, and might be part of the boundary of the basin of attraction of the stable operating condition.

In general the basin of attraction of the stable operating condition is expected to contain some singularity, either an unstable fixed point or an unstable periodic orbit. In the region of (p_1, p_2) control space satisfying inequalities (3), there are typically both stable and unstable periodic motions. For example, at $p_1 = 0.1$, $p_2 = 0.1$, we found three

stable periodic motions, corresponding to undesirable system operation (oscillation). It should be noted that a real generating system would not sustain these oscillations as our model does, since centrifugal forces would destroy the rotor.

By searching for fixed points in the surface of section $\delta_2 = 0$, we also found three unstable periodic motions. We have not yet tested whether the insets of these unstable periodic motions form part of any basin boundaries.

3. Basin Portraits

Figure 2 shows partial attractor-basin phase portraits of the coupled swing equations (1). In the upper left, Figure 2a is a section of the phase space in the (δ_1, δ_2) plane with $\omega_1 = \omega_2 = 0$. All initial conditions in the torus were integrated forward to determine whether the long-term behavior turned out to be the fixed point 1, or an oscillatory periodic attractor. An initial point leading to a periodic attractor is marked with a black dot, while an initial point in the basin of fixed point 1 is left unmarked. Another section of the same portrait in Figure 2b shows the (ω_1, ω_2) plane through the coordinates of fixed point 1, and the (δ_1, ω_1) and (δ_2, ω_2) sections in Figures 2c and 2d. We note that both fixed points 2 and 3 appear to lie in the basin boundary of the stable operating condition. We also checked that fixed point 4 lies in the basin boundary as well, although this is not so clear from Figure 2.

The global structure of this basin boundary appears to be complicated. To check whether fractal structure exists, a zoom sequence of successively magnified basin portraits was obtained inside the small square in Figure 2a. The results are shown in Figure 3, which con-

firms that the structure of the basin boundary is roughly the product of a one-dimensional Cantor-like set with a smooth three-dimensional surface. The structure would be typical of a transverse homoclinic intersection of a three-dimensional inset. Note however that even though the insets of fixed points 2 and 3 are three-dimensional, and they do intersect the two-dimensional outset of fixed point 4, they cannot have a transverse homoclinic intersection. It appears that unstable periodic motions generate tangles and the insets of fixed points 2 and 3 become involved with those tangles, perhaps following a structurally unstable homoclinic connection of Shilnikov type [**9**], or like that of the Lorenz system [**10**].

4. Control Space Portraits

Although the relationship between fixed points 2 and 3 and basin boundary of the stable operating condition is not simple, Figure 2 shows that the locations of these fixed points could be useful in devising approximate stability criteria. Indeed such approximations could be more accurate than stability criteria based on energy-integral or Lyapunov function approaches. Thus it might be of interest to know whether fixed point 2, for example, lies on this basin boundary for typical values of p_1 and p_2.

This question was studied numerically by following the outset branches of fixed point 2 for a large number of (p_1, p_2) values. The result is illustrated in Figure 4. A point in control space is marked with a black dot if exactly one branch of the outset of fixed point 2 leads to the stable operating condition; a gray dot means both branches lead to the stable fixed point; no dot indicates that both branches lead away.

The control space is thus divided into three regions. It appears that the structure of these regions is complicated. In the small square near the center of the triangular region in Figure 4, a zoom sequence showed an infinitely layered but not fractal structure. In the other small square in Figure 4, the zoom sequence shown in Figure 5 reveals an apparently fractal structure. Like the structure of the basin boundary near fixed point 2, this control region boundary seems to be roughly the product of a Cantor-like set with a three-dimensional smooth manifold.

5. Conclusions

In the study of transient stability dynamical systems, the attractor-basin phase portrait provides the most direct information about system stability. For example, if the system is subjected to an impulsive disturbance which effectively displaces the phase space coordinates from a stable condition to some other point, the system will regain the stable operating condition if and only if the perturbed point is in the basin of attraction of the stable operating condition.

Thus a direct numerical attack on the question of stability requires a systematic trial of many initial conditions and parameter values. Although such studies may require substantial computer time, they can in principle be carried out with any existing numerical model of system dynamics.

In interpreting the results of systematic trials, geometric phase portraits are essential tools. The presence of fractal structure should be expected, and the theory of invariant manifolds helps to understand and explain such structure. This requires numerical methods for locating unstable fixed points and unstable periodic motions of system

dynamics, such as straddle orbit algorithms [11] and push-pull algorithms [7].

The authors are grateful to the National Institute of Fusion Science at Nagoya for the use of the facilities of their Computer Center.

FIGURE CAPTIONS

1. Two machines operating onto an infinite bus system.
2. Partial basin portraits of coupled swing equations (1) with $p_1 = 0.1$, $p_2 = 0.1$ in sections of the four-dimensional phase space taken at $\omega_1 = 0$, $\omega_2 = 0$, δ_1 and /or δ_2 at the coordinates of fixed point 1; white regions are in the basin of attraction of the stable operating condition.
3. Magnification sequence of basin portrait section with $p_1 = 0.1$, $p_2 = 0.1$ showing fractal structure.
4. Control space portrait of position of fixed point 2 relative to the boundary of the basin of the stable operating condition, with black dots indicating regions where fixed point 2 is in the boundary.
5. Magnification sequence of the control space portrait in the small box near the corner of Figure 4, showing fractal structure.

Table 1. Coordinates and eigenvalues of fixed points for $p_1 = p_2 = 0.1$.

	fixed point 1	fixed point 2	fixed point 3	fixed point 4
δ_1	0.20136	0.20136	2.94023	2.94023
δ_2	0.30153	−3.04040	3.04040	−0.30153
eigen-values	−0.0250 + j5.0930	−4.0427	−2.4827	−5.1181
	−0.0250 − j5.0930	−0.0250 + j2.4574	−0.0250 + j4.0176	−1.9638
	−0.0250 + j1.9385	−0.0250 − j2.4574	−0.0250 − j4.0176	1.9138
	−0.0250 − j1.9385	3.9927	2.4327	5.0681

References

[1] A.H. El-Abiad and K. Nagappan, "Transient Stability Regions of Multimachine Power Systems", IEEE Trans. PAS-85, No. 2, pp. 169–179, Feb. 1966.

[2] P.D. Aylett, "The Energy-Integral Criterion of Transient Stability Limits of Power Systems", IEE Monograph No. 308s, pp. 527–536, July 1958.

[3] E. Carton and M. R-Pavella, "Lyapunov Methods Applied to Multimachine Transient Stability with Variable Inertia Coefficients", Proc. Iee, Vol 118, No. 11, pp. 1601–1606, Nov. 1971.

[4] J.M.T. Thompson, R.C.T. Rainey, and M.S. Soliman, *Ship stability criteria based on chaotic transients from incursive fractals*, Phil. Trans. Roy. Soc. A **332** (1990), 149–167.

[5] S.W. McDonald, C. Grebogi, E. Ott, and J.A. Yorke, *Fractal basin boundaries*, Physica **17D** (1985) 125.

[6] R. Thom, "Structural Stability and Morphogenesis". Benjamin: Reading, Mass., 1975.

[7] R.H. Abraham, *Dynasim: exploratory research in bifurcations using interactive computer graphics*. In "Bifurcation Theory and Applications in Scientific Disciplines", New York Academy of Sciences: New York, 1979.

[8] R.H. Abraham and C.D. Shaw, "Dynamics: The Geometry of Behavior, Parts I through IV". Aerial Press: Santa Cruz, Calif. 1982–88.

[9] J. Guckenheimer and P. Holmes, "Nonlinear Oscillations, Dynamical Systems, and Bifurcations of Vector Fields". Springer-Verlag: New York, 1983.

[10] J.M.T. Thompson and H.B. Stewart, "Nonlinear Dynamics and

Chaos". John Wiley and Sons: Chichester, 1986.

[11] P.M. Battelino, C. Grebogi, E. Ott, and J.A. Yorke, *Multiple coexisting attractors, basin boundaries, and basic sets*. Physica **32D** (1988) 296–305.

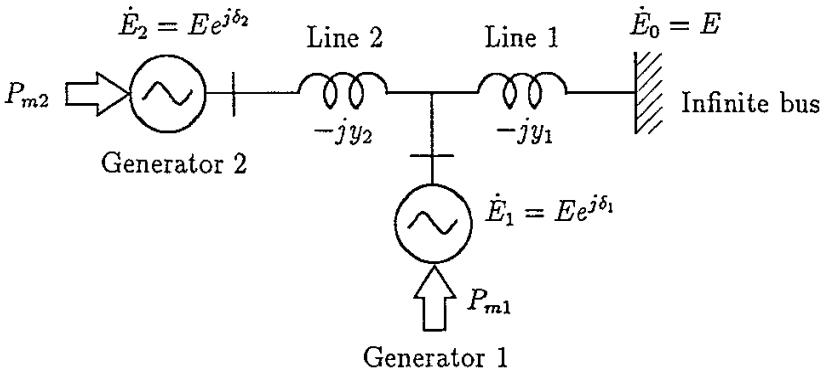
$\dot{E}_2 = Ee^{j\delta_2}$
Line 2
Line 1
$\dot{E}_0 = E$
P_{m2}
$-jy_2$
$-jy_1$
Infinite bus
Generator 2
$\dot{E}_1 = Ee^{j\delta_1}$
P_{m1}
Generator 1

Fig.1

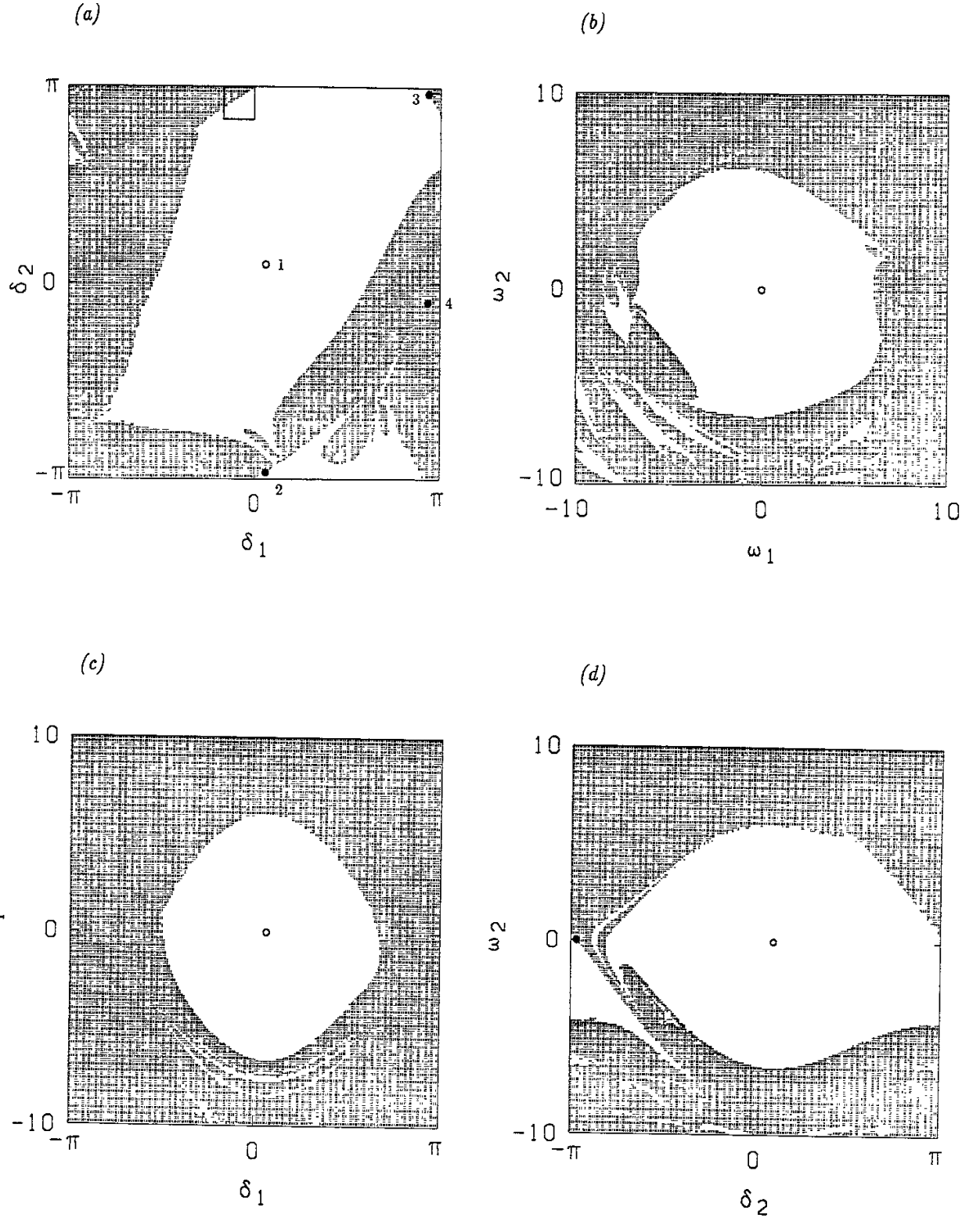

Fig.2

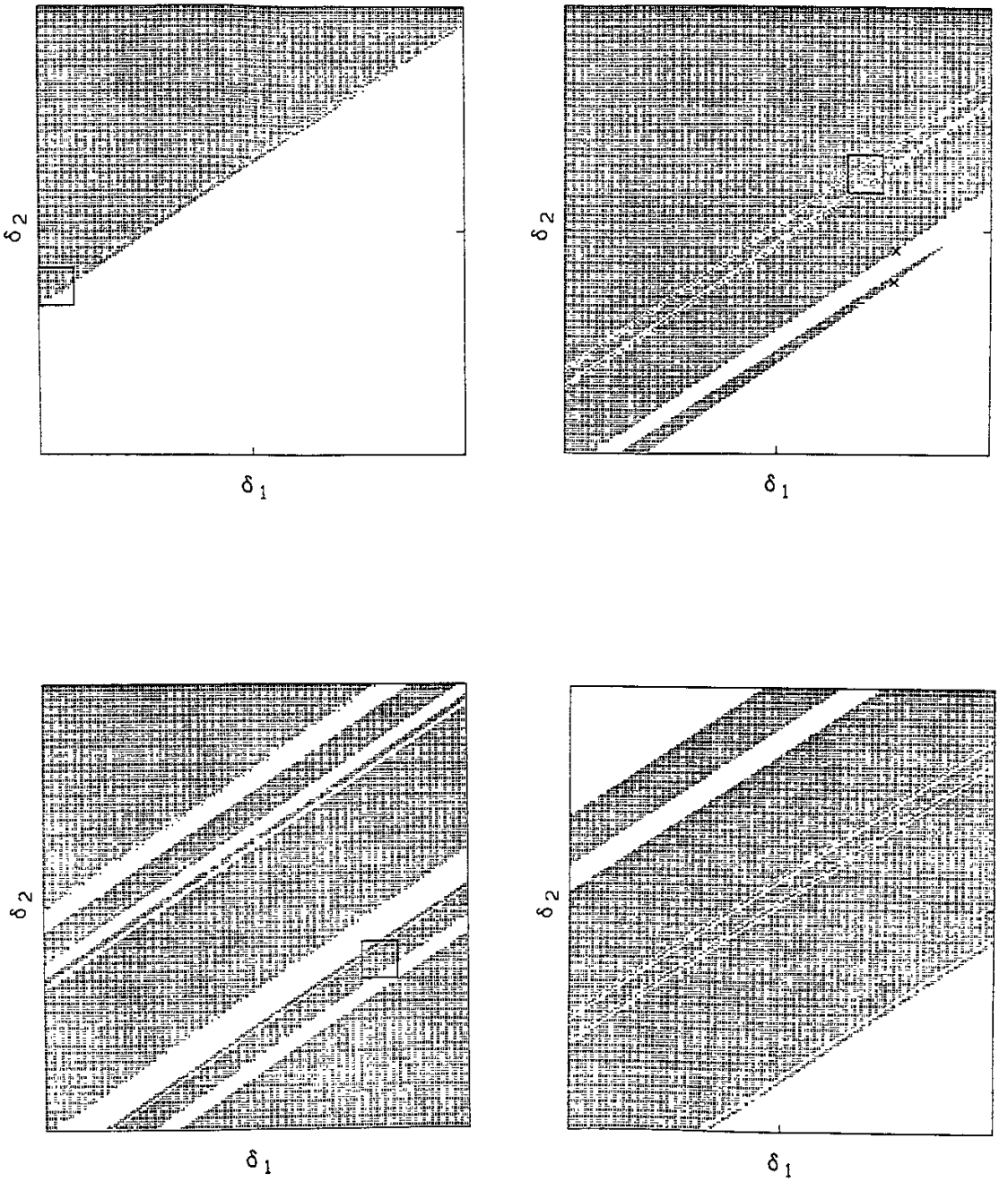

Fig.3

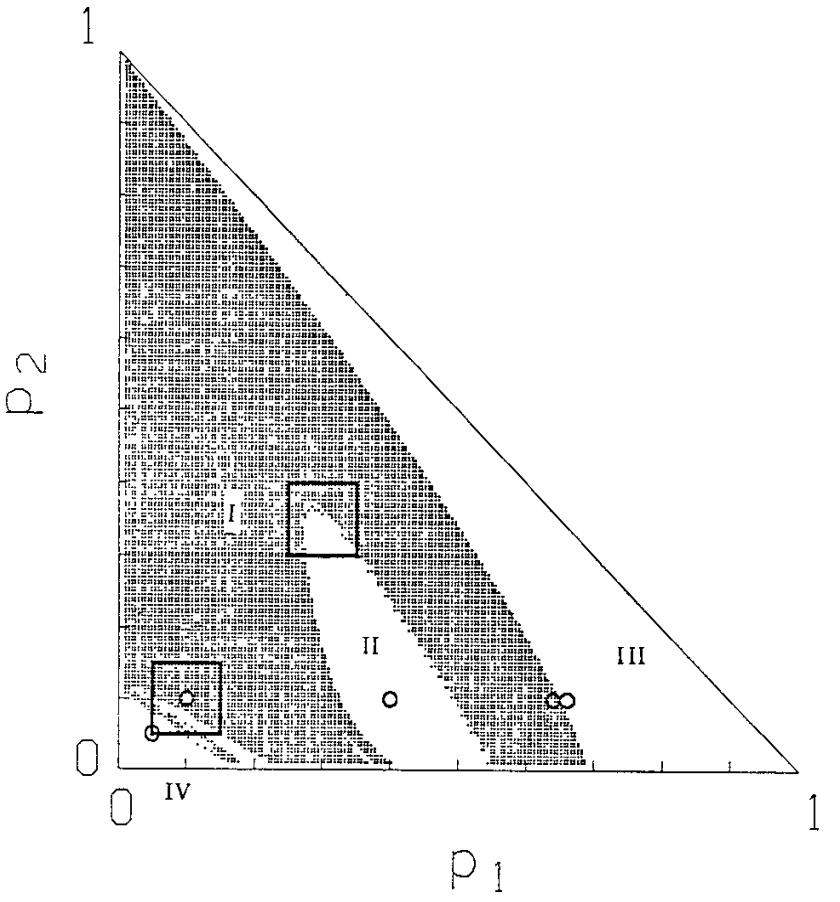

Fig.4

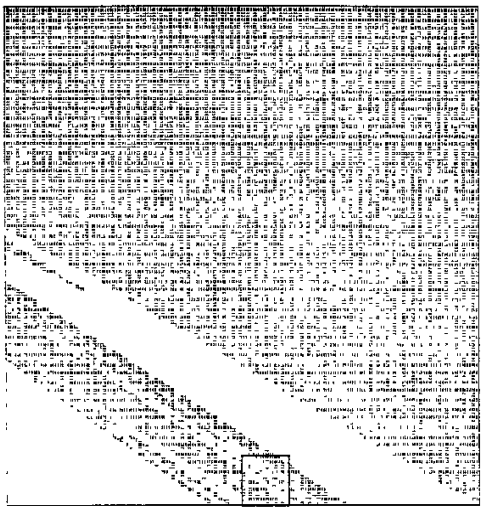

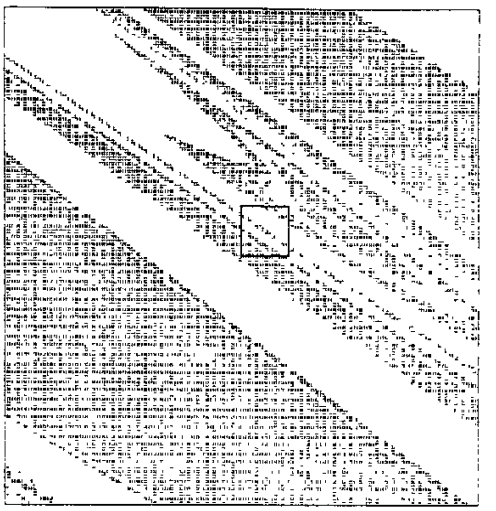

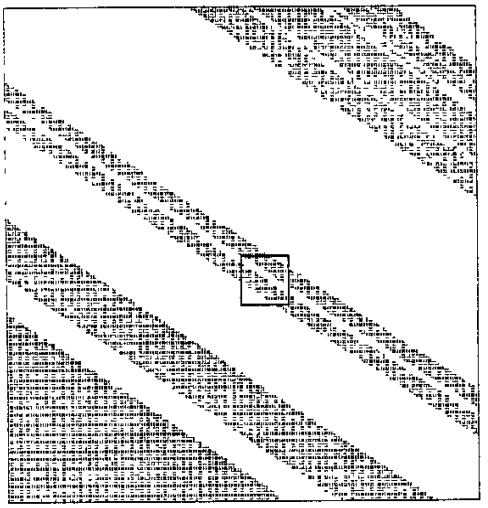

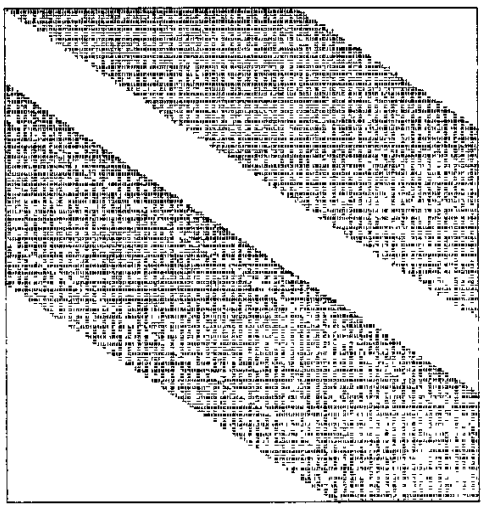

Fig.5